

# Dynamic Modeling and Verification of Litton's Space Inertial Reference Unit(SIRU) (ICCAS 2003)

Hong-Taek Choi. \*, Shi-Hwan Oh \*\* and Seung-Wu Rhee \*\*\*

- \* Korea Aerospace Research Institute, Yusung P.O.Box 113, Daejeon, 305-600 Korea  
(Tel : + 82-42-860-2808; E-mail : hongtaek@kari.re.kr)
- \*\* Korea Aerospace Research Institute, Yusung P.O.Box 113, Daejeon, 305-600 Korea  
(Tel : +82-42-860-2446; E-mail : oshwan@kari.re.kr)
- \*\*\* Korea Aerospace Research Institute, Yusung P.O.Box 113, Daejeon, 305-600 Korea  
(Tel : +82-42-860-2447; E-mail : srhee@kari.re.kr)

**Abstract:** Accurate mathematical models of spacecraft components are an essential of spacecraft attitude control system design, analysis and simulation. Gyro is one of the most important spacecraft components used for attitude propagation and control. Gyro errors may seriously degrade the accuracy of the calculated spacecraft angular rate and of attitude estimates due to inherent drift and bias errors. In order to validate this model, nominal case simulation has been performed and compared for the low range mode and high range mode, respectively. In this paper, a mathematical model of gyro containing the relationships for predicting spacecraft angular rate and disturbances is proposed.

**Keywords:** Attitude and Orbit Control Subsystem, Space Inertial Reference Unit, Angle White Noise, Angle Random walk, Noise Equivalent Angle, Space Inertial Reference Unit

## 1. INTRODUCTION

In this paper, Littons SIRU model with noise model for example satellite has been described. Gyro is one of the most important spacecraft components used for attitude propagation and control. Gyro errors may seriously degrade the accuracy of the calculated spacecraft angular rate and of attitude estimates due to inherent drift and bias errors. The general form of the model consists of physical plant equations, an error model, a stochastic model and a measurement model.

In order to validate this model, nominal case simulation has been performed and compared for the low range mode and high range mode, respectively

## 2. OVERALL SIRU CHARACTERISTICS

The performance characteristics for SIRU are summarized in Table 1.

Table 1 Key Performance Characteristics for SIRU

Parameter	Value
Rate Range(deg/sec)	+/- 10
Noise	
Noise Equivalent Angle(arc-sec)	3.0
Angle Random Walk(deg/hr^(1/2))	0.0003
Angle White Noise(arc-sec/Hz^(1/2))	0.014
Bias	
Tolerance over life(deg/h)	+/- 2.0
Stability, const temp(deg/hr, 1)	0.0006
Stability, 16 hrs w/+/- 10 deg C (deg/hr, pk)	0.015
Scale Factor	
Tolerance over life(%)	0.5
Stability, const temp(ppm, 1)	30
Stability, 16 hrs w/+/- 10 deg C (ppm, pk)	300

Linearity(deg/hr, pk)	0.8
Resolution(arc-sec/LSB)	0.05
Bandwidth(Hz at 3 db)	7

## 3. GYRO MODELING

In this section, mathematical models for the estimation of spacecraft angular rate from gyro measurements, the simulation of gyro outputs from true spacecraft angular rate and the modeling of noise in gyro outputs is described. For the rate integrating gyro, measurement of the average angular velocity over the interval is

$$\varpi_i^M = \frac{K_I \theta_I}{\delta t_I} \quad (1)$$

where  $K_I$  is the rate integrating scale factor,  $\delta t_I$  is sampling interval and  $\theta_I$  is the gyro output.

The spacecraft angular velocity  $\varpi_i$  is related to the gyro's measurement angular velocity and becomes

$$\varpi_i^M = (1+k_i)\varpi_i + b_i + n_i \quad (2)$$

where  $k_i$  is a small correction to the nominal scale factor.  $b_i$  is the drift rate and  $n_i$  is white noise on the gyro output. In torque rebalanced gyros,  $b_i$  represents a null shift in the torque rebalance control loop. In the direction of the gyro's input axis is given by a unit vector,  $\hat{U}_i$ , in the spacecraft coordinate frame, Eq. (2) becomes

$$\varpi_i^M = (1+k_i)\hat{U}_i \cdot \vec{\omega} + b_i + n_i \quad (3)$$

where  $\vec{\omega}$  is the true spacecraft angular velocity vector.

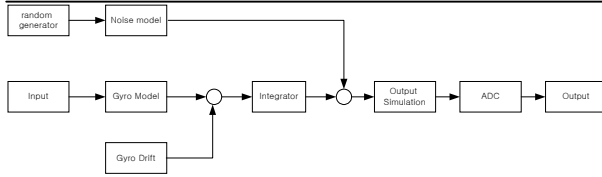


Fig. 1 The Block diagram for the General Gyro Model

Fig. 1 shows the block diagram for the general gyro model. In this block diagram, all block except noise model consists of simple function. Noise model is more complicate than other model. Random generator generates triple precision gaussian random number which has a normally distributed random number with zero mean and unit standard deviation. Noise model can be described by transfer function in continuous time system and transformed into state space in discrete time system. Input for gyro model is the body rate in gyro frame transformed from in body frame. The body rate in gyro frame is transformed into four gyro axis. Gyro dynamics is described as 2nd order low pass filter. Gyro drift is modeled as a constant rate. The sum of gyro rate and gyro drift and gyro drift is changed to angular change by integration. The sum of angular change and noise is the total angle by gyro. The angle is transformed into count multiplying by scale factor. When the angle changes to counter by 16 bit counter, the residual angle is generated. The residual angle is summed up next cycle angle. The angle is limited to minimum angle and maximum angle. Whenever the gyro angle is out of range, the gyro counter is roll over. The gyro model output is the count and is limited from 0 to 65535.

#### 4. CONTROLLER DESIGN RESULTS

In this section, it is developed to provide test inputs and expected results and data collecting and reporting requirements. In order to verify gyro processing logic and gyro model, the test profile of angular velocity is set up in gyro box coordinate in low rate range mode and in high rate range mode for the gyro model.

##### 4.1 Low rate Range Mode

It is considered that the amplitude of test profile is 2.5 deg/sec to present rate saturation in low rate range mode and the frequency is about 105 times of the frequency of satellite, that is  $1.068 \times 10^{-3}$  rad/sec.

$$\begin{aligned} W\_gyro[0] &= 2.5 \cdot 3.14 / 180 \cdot \sin(1.068 \cdot 105 \cdot e^{-3} \cdot t) \\ W\_gyro[1] &= 2.5 \cdot 3.14 / 180 \cdot \cos(1.068 \cdot 105 \cdot e^{-3} \cdot t) \\ W\_gyro[2] &= 0.0 \end{aligned}$$

Fig. 2 shows the test profile in roll, pitch and yaw axis in 100 sec. This test profile should be transformed into angular velocity in gyro coordinate. The angular velocity of each gyro shall be integrated for the sampling time to generate the

accumulated angle. The sampling time in this gyro model is regarded as constant of 0.25 sec of the program update time.

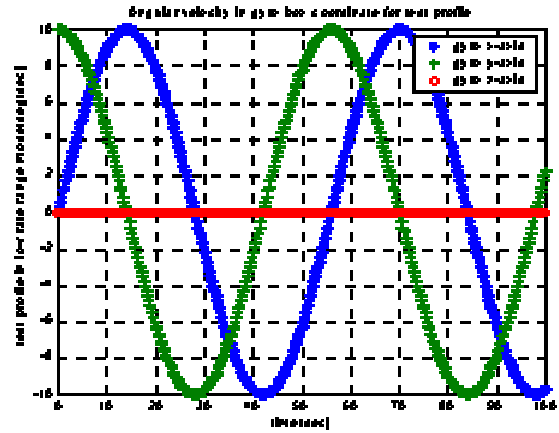


Fig. 2 Angular Velocity in Gyro Frame for Test Profile in Low Rate Range Mode

Fig. 3 presents the angle for each gyro in gyro axis coordinate. As we expected, the gyro 4 shows the zero angle. The amplitude is reduced by a factor of about 0.05 for gyro1, gyro2 and gyro3 and the frequency is following the same as original test profile. The following equation shows the relationships between gyro box and each gyro configuration.

$$W_{abcd} = \begin{bmatrix} 0 & -\frac{\sqrt{2}}{3} & -\frac{\sqrt{1}}{3} \\ \frac{\sqrt{2}}{2} & \frac{\sqrt{2/3}}{2} & -\frac{\sqrt{1}}{\sqrt{3}} \\ -\frac{\sqrt{2}}{2} & \frac{\sqrt{2/3}}{2} & -\frac{\sqrt{1}}{\sqrt{3}} \\ 0 & 0 & 1 \end{bmatrix} * W_{gyro} \quad (4)$$

The accumulated angle is converted into gyro counts after checking the roll off associated with 16 bit quantization.

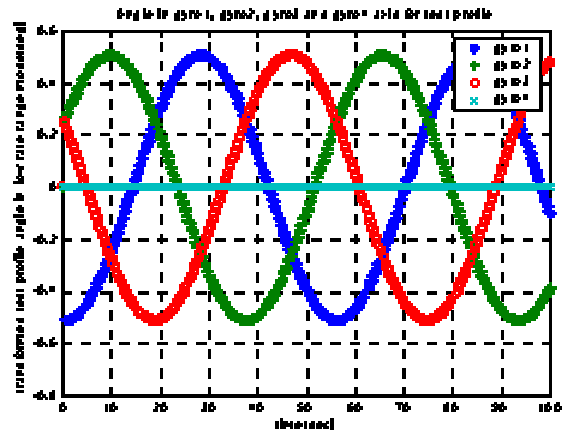


Fig. 3 Transformed Angle in Gyro Axis Frame including Noise for Test Profile

Fig. 4 presents the magnified counts for each gyro in low rate range mode for test profile during 25 sec to 50 sec. It shows the wrap around but it seems to be difficult to derive the relation with gyro angle in that it rolls over very quickly. If the rate is changed slowly, it can show more realistic roll over profile. It will be shown later.

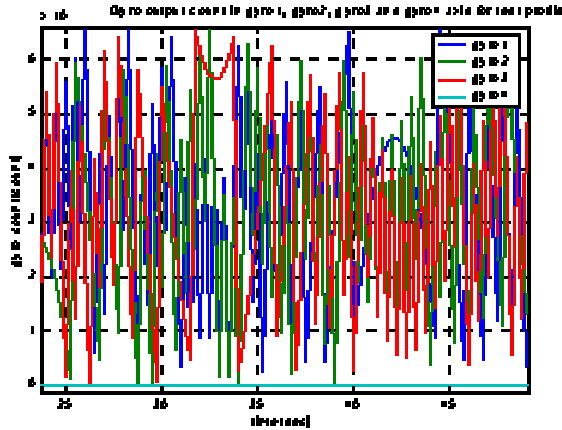


Fig. 4 Gyro Counts in Gyro Axis Frame in Gyro Model for test profile

Fig. 5 shows the angle in gyro axis frame derived in gyro data processing transformed from gyro counts in gyro model. This test profile should also be transformed into angular velocity in gyro coordinate. It shows the same as the transformed profile in gyro model except the saturation. Whenever gyro angle in gyro model is greater than 0.45 deg, it shows the saturation which affects the angle in gyro data processing.

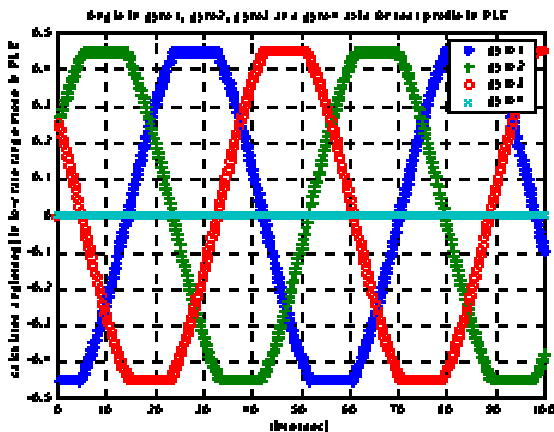


Fig. 5 Calculated Gyro Angle in Gyro Axis Frame in Gyro Data Processing Logic

Fig. 6 shows the difference angle between transformed angle in gyro axis frame in gyro model and calculated angle in gyro axis angle in gyro data processing logic. The maximum difference angle is within about 0.6 arcsec. The gyro 1 is not shown since it is saturated in this region. The difference is caused by the noise equivalent angle and quantization error.

This data can be compared with the noise equivalent angle directly derived from noise model shown in the last part.

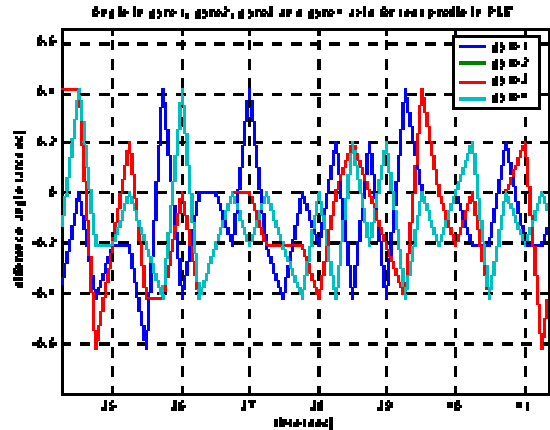


Fig. 6 Difference Angle between Calculated Gyro Angle in Gyro Axis Frame and in Gyro Data Processing Logic

#### 4.2 High rate Range Mode

Similarly, it is considered that the amplitude of test profile is 10 deg/sec to present rate saturation in high rate range mode and the frequency is about 105 times of that of KOMPSAT-2, that is  $1.068 \times 10^{-3}$  rad/sec.

$$W\_gyro[0] = 10 \times 3.14 / 180 \times \sin(1.068 \times 105 \times e^{-3} \times t)$$

$$W\_gyro[1] = 10 \times 3.14 / 180 \times \cos(1.068 \times 105 \times e^{-3} \times t)$$

$$W\_gyro[2] = 0.0$$

Fig. 7 shows the test profile in roll, pitch and yaw axis in 100 sec. This test profile is also transformed into angular velocity in gyro coordinate. The sampling time in this gyro model is regarded as constant of 0.25 sec of the program update time.

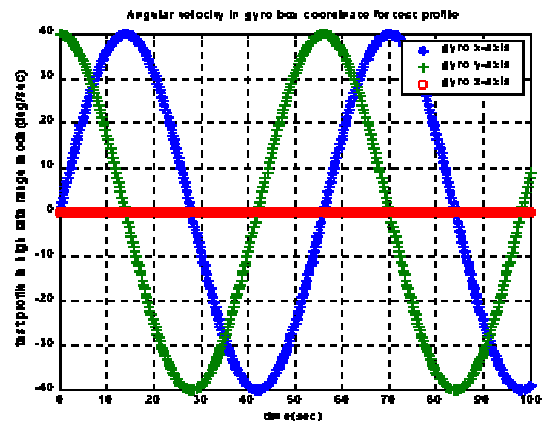


Fig. 7 Angular Velocity in Gyro Frame for Test Profile in High Rate Range Mode

Fig. 8 presents the angle for each gyro in gyro axis coordinate. As we expected, the gyro 4 shows the zero angle. The amplitude is reduced by a factor of about 0.05 for gyro1, gyro2 and gyro3 and the frequency is following the same as

original test profile. The accumulated angle is converted into gyro counts after checking the roll over associated with 16 bit quantization.

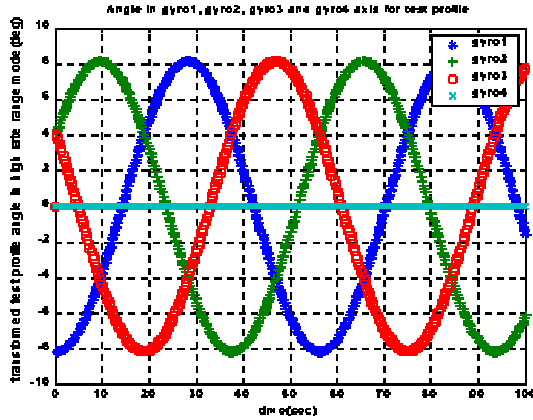


Fig. 8 Transformed Angle in Gyro Axis Frame including Noise for Test Profile

Fig. 9 presents the magnified counts for each gyro in low rate range mode for test profile during 25 sec to 50 sec. It shows the similar wrap around and profile compared to low range mode.

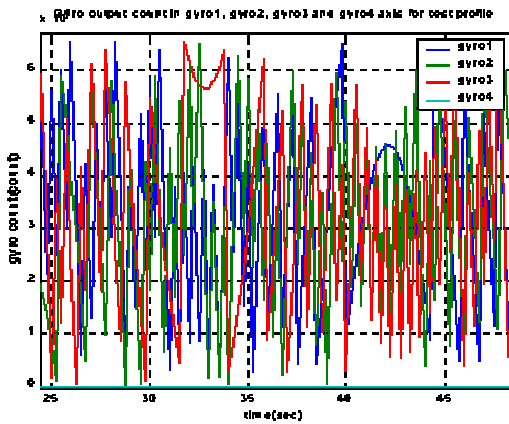


Fig. 9 Gyro Counts in Gyro Axis Frame in Gyro Model for test profile

Fig. 10 shows the angle in gyro axis frame derived in gyro data processing transformed from gyro counts in gyro model. Compared to low rate range mode, the amplitude increased 4 times but the frequency is the same as we expected. It also shows the same as the transformed profile in gyro model except the saturation. Whenever gyro angle in gyro model is greater than about 1.8 deg, it shows the saturation which affects the angle in gyro data processing.

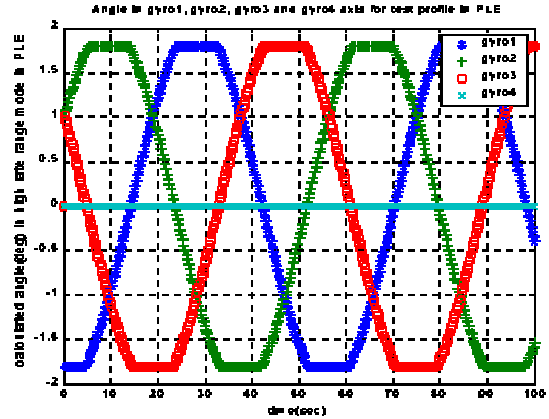


Fig. 10 Calculated Gyro Angle in Gyro Axis Frame in Gyro Data Processing Logic

Fig. 11 shows the difference angle between transformed angle in gyro axis frame in gyro model and calculated angle in gyro axis angle in gyro data processing logic. The maximum difference angle is within about 2.0 arcsec. The gyro 2 is not shown since it is saturated in this region. It also shows that the difference angle is greater compare to in the low range mode.

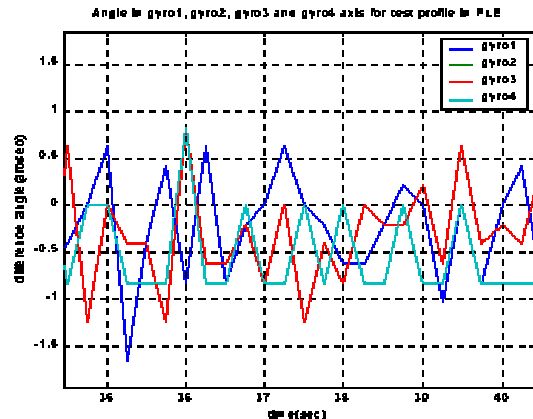


Fig. 11 Difference Angle between Calculated Gyro Angle in Gyro Axis Frame and in Gyro Data Processing Logic

Next, we presents angular velocity in gyro frame for new test profile. The x-axis rate increases with constant inclination while y-axis rate and z-axis rate is zero as it is expected. The test profile is as follows:

$$\begin{aligned}
 W\_gyro[0] &= 0.05 * 3.14 / 180 * \text{current\_time} \\
 W\_gyro[1] &= 0.0 \\
 W\_gyro[2] &= 0.0
 \end{aligned}$$

Fig. 12 shows the gyro count derived from each gyro angle. Gyro 2 has the increased count and gyro 3 has the decreased count as it is expected. To present roll over, the count has the value between 0 and 65535(unsigned 16 bit). Gyro angle for each gyro is compared with gyro angle results from gyro counts. It is expected that gyro 4 to measure the rate of z-axis

is zero counts or zero rate considering the gyro configuration and yaw axis angular velocity of the test profile. The period of roll over is about 5 sec.

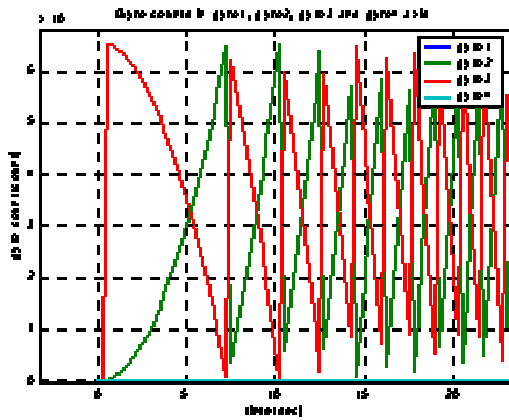


Fig. 12 Gyro Count derived from Each Gyro Angle

Fig. 13 shows the calculated gyro angle in gyro data processing logic. Gyro 2 and gyro 3 show the saturation after about 50 sec.

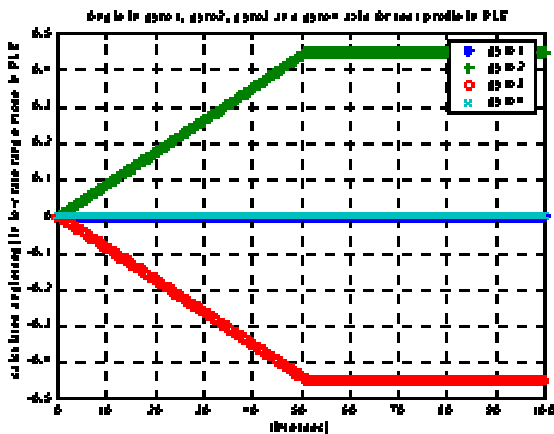


Fig. 13 Calculated Gyro Angle in Gyro Data Processing Logic

Fig. 14 shows the noise equivalent angle. The NEA for this gyro is shown to be 0.6 arc-seconds. NEA consists of white noise(AWN) including quantization noise, angle random walk(ARW) and rate flicker.

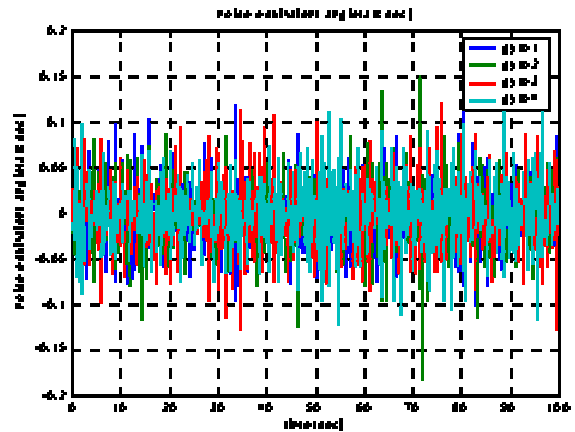


Fig. 14 Noise Equivalent Angle for Each Gyro

### 5. CONCLUSIONS

In this paper, the gyro model used for example satellite is checked to provide the assurance of the gyro model validation. However, it may be possible to find the error executing gyro model with implementation it into whole example satellite simulation.

### REFERENCES

- [1] SIRU Technical Description for Matra Marconi
- [2] SIRU Retro-Specification
- [3] SIRU Installation Control Drawing
- [4] IEEE Standard Specification format Guide and Test, Std 647-1995
- [5] Litton Guidance & Control systems "SIRU-Core technical Description"
- [6] James R. Werthz, Spacecraft Attitude Determination and Control, D. Reidel Publishing Company, 1986